Membrane Water Treatment, *Vol. 8, No. 1 (2017) 89-112*
DOI: https://doi.org/10.12989/mwt.2017.8.1.089

Pre-treatment of textile wastewaters containing Chrysophenine using hybrid membranes

Arash Yunessnia lehi*[1], Seyed Jalaleddin Mousavirad[2a] and Ahmad Akbari[1,3b]

[1]*Institute of Nanoscience and Nanotechnology, University of Kashan, P.O. Box: 87317-53153, Kashan, Iran*
[2]*Department of Computer Engineering, Faculty of Computer & Electrical Engineering, University of Kashan, Kashan, Iran*
[3]*Department of Carpet, Faculty of Architecture & Art, University of Kashan, Kashan, Iran*

(*Received November 12, 2015, Revised November 5, 2016, Accepted November 15, 2016*)

Abstract. Dyeing wastewaters are the most problematic wastewater in textile industries and also, growing amounts of waste fibers in carpet industries have concerned environmental specialists. Among different treatment methods, membrane filtration processes as energy-efficient and compatible way, were utilized for several individual problems. In this research, novel hybrid membranes were prepared by waste fibers of mechanical carpets as useful resource of membrane matrix and industrial graphite powder as filler to eliminate Chrysophenine GX from dyeing wastewater. These membranes were expected to be utilized for first stage of hybrid membrane filtration process including (adsorption-ultrafiltration) and nanofiltration in Kashan Textile Company. For scaling of membrane filtration process, fouling mechanism of these membranes were recognized and explained by the use of genetic algorithm, as well. The graphite increased rejection and diminished permeate flux at low concentration but in high concentration, the performance was significantly worsened. Among all hybrid membranes, 18% wt. waste fibers-1% wt. graphite membrane had the best performance and minimum fouling. The maximum pore size of this optimum membrane was ranged from 16.10 to 18.72 nm.

Keywords: chrysophenine GX; fouling mechanisms; genetic algorithm; hybrid membranes; wastage fibers

1. Introduction

Among all sources of wastewater in textile industry, dyeing wastewaters are the most problematic due to the existence of dyes. These dyes usually have complex aromatic structures and can be very toxic. Also, they are stable to light, oxidizing agents and aerobic digestion. Among these dyes, the anionic dyes are found to be the brightest sort of soluble dyes, which can be caused serious environmental and health problems (Akbari, Remigy *et al.* 2002a, Khaled, El Nemr *et al.* 2009, Ghaedi, Sadeghian *et al.* 2012). Chrysophenine GX (Direct Yellow 12) belongs to azo and

∗Corresponding author, Ph.D., E-mail: arash_yunessnia_lehi@yahoo.com
[a]Ph.D., E-mail: jalalmoosavirad@gmail.com
[b]Ph.D., E-mail: akbari@kashanu.ac.ir

 ISSN: 2005-8624 (Print), 2092-7037 (Online)

anionic dyes category that widely applied in industries such as dying silk and wool, biological stains and green ink manufacture. It has high biological oxygen demand (BOD) and is stable in both acidic and alkali mediums (Khaled, El Nemr *et al.* 2009, Rathi, Rajor *et al.* 2003). Existing of this dye in the aquatic environment can be caused permanent injury in humans and animals eyes (Rathi, Rajor *et al.* 2003, Ghaedi, Sadeghian *et al.* 2013). Therefore, treatment of wastewaters containing this dye is a challenging requirement. For having good result, the treatment processes had to reduce the dye more than 90% (Akbari, Desclaux *et al.* 2007).

Treatment technologies for removing this anionic dye from wastewater are divided into several groups such as adsorption (Khaled, El Nemr *et al.* 2009, Ghaedi, Sadeghian *et al.* 2012, Ghaedi, Sadeghian *et al.* 2013, Revathi, Ramalingam *et al.* 2011), biosorption (Said, Aly *et al.* 2013, El Nemr, Abdelwahab *et al.* 2006), biological treatment (Van der Zee, Lettinga *et al.* 2001), photochemical treatment (Rathi, Rajor *et al.* 2003, Sohrabi and Ghavami 2010), photoelectrochemical treatment (Khataee and Zarei 2011) and other methods (Abedi and Nekouei 2011). There are advantages and disadvantages associated with each of these techniques, but all of them are not commercially suitable for Chrysophenine GX. For instance, the azo dye is reduced to colorless primary amines in conventional biological treatment and they are even more toxic than the original dye (Rathi, Rajor *et al.* 2003, El Nemr, Abdelwahab *et al.* 2006, Van der Zee, Lettinga *et al.* 2001).

For efficient treatment processes, some environmental scientists have been attracted to membrane techniques. The membrane filtration can be potentially used for the removal of dyes without degradation of them. Also, these techniques allow concentration of dyes and reuse of them (Akbari, Remigy *et al.* 2002a, Akbari, Desclaux *et al.* 2002b, 2006, 2007, Purkait, DasGupta *et al.* 2004, Kurt, Koseoglu-Imer *et al.* 2012, Aouni, Fersi *et al.* 2012, Van der Bruggen, Curcio *et al.* 2004). For example, Purkait, DasGupta *et al.* (2004) used ultrafiltration to remove an acid dye from aqueous solution, using CPC as a cationic surfactant and polyamide membrane. The retention of dye without using surfactant was only 10% while under the same operating pressure, retention was increased up to 73.4% by using surfactant micelles. Also, Akbari, Remigy *et al.* (2002a) investigated the performance of a commercial polyamide nanofiltration membrane in treating colored textile effluent. In this study, Direct Red 80 and Direct Yellow 8 were retained 100% and make them suitable for reuse.

However, the major problem with all membrane filtrations is the decline of permeation fluxes due to the accumulation of molecules on the membrane surface (Goosen, Sablani *et al.* 2005, Gao, Liang *et al.* 2011, Koyuncu, Topacik *et al.* 2004, Van der Bruggen, Curcio *et al.* 2005). This process is known as concentration polarization and leads to a membrane fouling. There are some recommended methods to decrease fouling for the treatment of textile wastewater:

1- Using consecutive or combined processes to remove different species or to lessen their concentrations before the main filtration (i.e., hybrid processes) (Van der Bruggen, Curcio *et al.* 2004, Allègre, Moulin *et al.* 2006). Examples include ultrafiltration + nanofiltration (Fersi and Dhahbi 2008), nanofiltration + reverse osmosis (Kurt, Koseoglu-Imer *et al.* 2012, Nataraj, Hosamani *et al.* 2009) and microfiltration + coagulation + adsorption (Lee, Choi *et al.* 2006).

2- The incorporation of porous or nonporous inorganic absorbents into the membranes to achieve high permeability and selectivity values for membrane filtration processes (i.e., hybrid membranes) (Kim and Van der Bruggen 2010). The permeability of these hybrid membranes depends on the intrinsic properties of inorganic material and polymer and the interaction between the two phases. Also, the inorganic content and particle size can affect the permeability of these hybrid membranes (Peng, Lu *et al.* 2007). Some examples of these absorbents include

zeolites (Fathizadeh, Aroujalian *et al.* 2011, Huang, Qu *et al.* 2013), clay (Adoor, Sairam *et al.* 2006), TiO_2 nanoparticles (Li, Xu *et al.* 2009, Li, Zhu *et al.* 2007), carbon nanotubes (Shi, Zhang *et al.* 2013, Gethard, Sae-Khow *et al.* 2010, Kim, Choi *et al.* 2014), graphite (Peng, Lu *et al.* 2005, 2007, Prusty and Swain 2011, Yakovlev, Finaenov *et al.* 2004) and activated carbon (Ballinas, Torras *et al.* 2004, Torras, Ferrando *et al.* 2006, Hwang, Chen *et al.* 2013).

3- The grafting of various hydrophobic monomers on the membrane surface to enhance their fouling resistance during the filtration. Some of these materials include acrylamide, methacrylic acid and 3-sulfopropyl methacrylate (Reddy, Trivedi *et al.* 2005) and poly(ethylene glycol) methyl ether acrylate (Asatekin, Olivetti *et al.* 2009).

Unfortunately, the number of studies about the treatment of wastewater containing Chrysophenine GX molecules using membrane filtration was very limited. As a part of ongoing research program in the laboratory of Akbari *et al*., we attempted to prepare and evaluate a hybrid ultrafiltration membrane with the lowest degree of fouling in the early time of process. These membranes will be used for the first stage of a hybrid membrane filtration process consisting of adsorption, ultrafiltration and nanofiltration to remove Chrysophenine GX. Chrysophenine GX is consumed for cotton dyeing in Kashan Textile Company and this investigation is applied for wastewater treatment unit in this company. In order to prepare this hybrid membrane, we use waste fibers of mechanical carpets and industrial graphite powder.

During fabrication of mechanized carpet by carpet industries, a large amount of fibers are wasted that could be used for other applications. The waste fibers of mechanized carpet were used for enhancing the strength properties of granular soils (Shahnazari, Ghiassian *et al.* 2009, Mirzababaei, Miraftab *et al.* 2013) and reinforcing several kinds of composites (Taşdemır, Koçak *et al.* 2007). These waste fibers are an inexpensive copolymer of polyacrylonitrile consist of >85% acrylonitrile and other monomers. Polyacrylonitrile is one of the popular membrane materials for water and wastewater treatment, because of sufficient chemical stability, hydrophilicity and good solubility in common solvents. It is also known as a low fouling membrane for aqueous filtration (Lohokare, Bhole *et al.* 2011).

As an inorganic absorbent, graphite powder was chosen based on the following considerations: 1- Graphite has higher flexibility, appreciable mechanical properties, low density, easy processing and relatively low cost (Prusty and Swain 2011). 2- Graphite is hydrophobic with uniform electron distributions and when it is added into the membrane, it changes the chemical properties, porosity, and filtration flux of membrane (Hwang, Chen *et al.* 2013). 3- Graphite is one of the candidate materials used to show affinity toward aromatics (Lu, Sun *et al.* 2006). 4- Oxygen can be chemisorbed on the surface of graphite, thereby can be ensured to have a positive potential when it is subsequently incorporated in the membrane (Yakovlev, Finaenov *et al.* 2004).

Furthermore, membrane properties including water permeability, rejection, membrane structure and surface roughness were characterized for the interpretation of performance differences between these hybrid membranes. Also, genetic algorithm was used for the evaluation of fouling mechanisms (Soleimani, Shoushtari *et al.* 2013, Okhovat and Mousavi 2012, Sahoo and Ray 2006).

2. Experimental

2.1 Materials

Waste fibers of mechanical carpets were supplied by Paitakht Carpet Company (Kashan, Iran,

Fig. SI 1A). N, N-dimethylformamide (DMF, MW=73.09 g/mol, industrial grade) was purchased from Kimia Zist Azma Company (Tehran, Iran). Graphite powder (1 μm, Fig. SI 1B) was bought from local company (Tehran, Iran). Deionized water was also used as non-solvent agent in the coagulation bath. Chrysophenine GX (Direct Yellow 12) with MW=680.66 g/mol (Color Index: 24895) was supplied by Alvan Sabet Company (Hamedan, Iran) and used as textile dye for the preparation of feed solutions in the dye rejection experiments.

2.2 Membrane preparation

Firstly, the graphite powder was dispersed in DMF at 40±2℃ for 30 minutes by ultrasonic water bath (Bandelin DT 255H, Germany). Afterwards, different amount of cleaned waste fibers were prepared and added to graphite mixtures. The mixtures were magnetically stirred at temperature of 80±2℃ for at least one day. Subsequently, the prepared homogeneous solutions were cast by the use of a film applicator to 350 μm clearance gap on a glass plate substrate. Temperature and relative humidity of casting environment were ~24℃ and 23%, respectively. The cast films were immediately immersed in a deionized water bath at room temperature to complete phase separation. In order to reduce the effect of unexpected variability and obtain the best membrane performance, this procedure was done three times.

2.3 Membrane characterization and performance

Morphology of the dried membranes was examined using scanning electron microscopy (SEM, KYKY-EM3200 and Hitachi S-4160) and atomic force microscopy (AFM, Solver PRO, Russia). FT-IR spectroscopy (Nicolet Magna IR 550) was accomplished for the qualitative analysis of initial materials and hybrid ultrafiltration membranes. Pore size distribution of optimum membrane was measured using N_2 adsorption porosimetry (NOVA 2000 version 7.11, QuantaChrome Corporation, USA). Permeation flux experiments were performed by an ultrafiltration setup that was conducted in cross-flow mode. It offered an effective filtration area of 32 cm^2, a tangential feed flow on the membrane surface of 4.5 L/min, a pressure of 4 bar and an operating temperature of 27±2℃. These experiments were applied for three membranes. For the measurement of rejection, the concentrations of Chrysophenine GX in feeds were kept constant at 100 ppm in all experiments. Also, the concentration of solutions in feeds and permeations were measured by UV-Vis spectrophotometer (λ_{max}=400 nm, GBC model Cintra 101, Australia).

2.4 Parameter estimation using genetic algorithm

In the genetic algorithm, each solution is shown by an array which is called chromosome. Each chromosome is a string of floating point number which is shown by the equation parameters. First, a population of candidate solutions is created randomly. In each generation, the fitness of every chromosome in the population is evaluated. The fitness of a chromosome is defined as the mean square error (MSE). Then in the selection process, chromosomes with higher fitness have a higher probability to be selected. The next step is to generate the new chromosome using crossover and mutation operator. In crossover operator, two chromosomes are selected and two new chromosomes are generated from them. The mutation operator generates one new chromosome from old chromosome by changing one or more parts of a chromosome. This iterative process continues until the termination condition is reached. In this paper, the process stopped if the

Table 1 Fouling mechanistic models for cross-flow filtration processes

Models	Flux-Time relationship	Ref.
Power Law Model (PLM)	$J = J_0 t^{-k}$	Kuo and Cheryan (1983) Fane and Fell (1987)
Pore Blockage Model (PBM)	$J = \left(J_0 - J^*\right)\exp\left[-\frac{J_0 \alpha C_b}{N_0 \pi r_p^2} t\right] + J^*$	
Pore Constriction Model (PCM)	$J = J^*\left[\frac{\left[1+\frac{\sqrt{J_0}-\sqrt{J^*}}{\sqrt{J_0}+\sqrt{J^*}}\exp\left(-\frac{2\sqrt{J_0 J^*}\alpha_b A_m C_b}{\pi r_0^2 \delta_m} t\right)\right]}{\left[1-\frac{\sqrt{J_0}-\sqrt{J^*}}{\sqrt{J_0}+\sqrt{J^*}}\exp\left(-\frac{2\sqrt{J_0 J^*}\alpha_b A_m C_b}{\pi r_0^2 \delta_m} t\right)\right]}\right]^2$	Kilduff, Mattaraj *et al*. (2002) Field and Wu (2011)
Cake Formation Model (CFM)	$\frac{1}{J^{*2}}\left(\left[\ln\frac{J\left(J_0 - J^*\right)}{J_0\left(J - J^*\right)}\right] - J^*\left(\frac{1}{J}-\frac{1}{J_0}\right)\right) = \frac{\alpha_c A_m C_b}{J_0 R_m} t$	

generation number was greater than 200. The fouling mechanism models of cross-flow filtration processes are shown in Table 1, their parameters were achieved through genetic algorithm.

3. Results and discussion

3.1 SEM analysis

In order to investigate the separation of Chrysophenine GX using waste fibers/graphite hybrid ultrafiltration membranes, dope solutions were firstly prepared with 16, 18 and 20% wt. The concentration of waste fibers and the structure and performance of formed membranes were carefully examined. Fig. 1(a) shows the cross-section image of membrane with 16% wt. waste fibers, for instance. As expected, the addition of waste fibers concentration increased viscosity of dope solution (Lohokare, Bhole *et al.* 2011, Shinde, Kulkarni *et al.* 1999, Yang and Liu 2003). As a consequence, it could severely hinder the exchange rate or diffusive mass transfer of DMF and water during phase separation process and could affect the precipitation kinetics. In other words, the growth rate and amount of polymer poor phases (pores) were diminished in the forming membranes (Yang and Liu 2003). In this image, very small finger-like and macrovoid structures can be observed in the top dense layer that was illustrated by Lohokare, Bhole *et al.* (2011). Also, a fused nodular structure was well developed in the rim of macrovoids (Fig. SI 2). By increasing of waste fibers concentration, the numbers of these nodular structures have increased, but their sizes have decreased. As suggested by Smolders, Reuvers *et al.* (1992), the spherical structure is presumably related to the clustering of entanglement of polymer molecules during spinodal decomposition (Jung, Yoon *et al.* 2004, Yunessnia lehi, Akbari *et al.* 2013).

Incorporation of graphite powder with different content into waste fiber ultrafiltration membranes strongly affects membrane properties. This has occurred in two regions, i.e., <6% and >6% wt. because of the interaction among graphite powder, waste fiber, solvent and non-solvent (Peng, Lu *et al.* 2005, 2007, Lu, Sun *et al.* 2006). When 1%wt. or 3% wt. graphite was added to

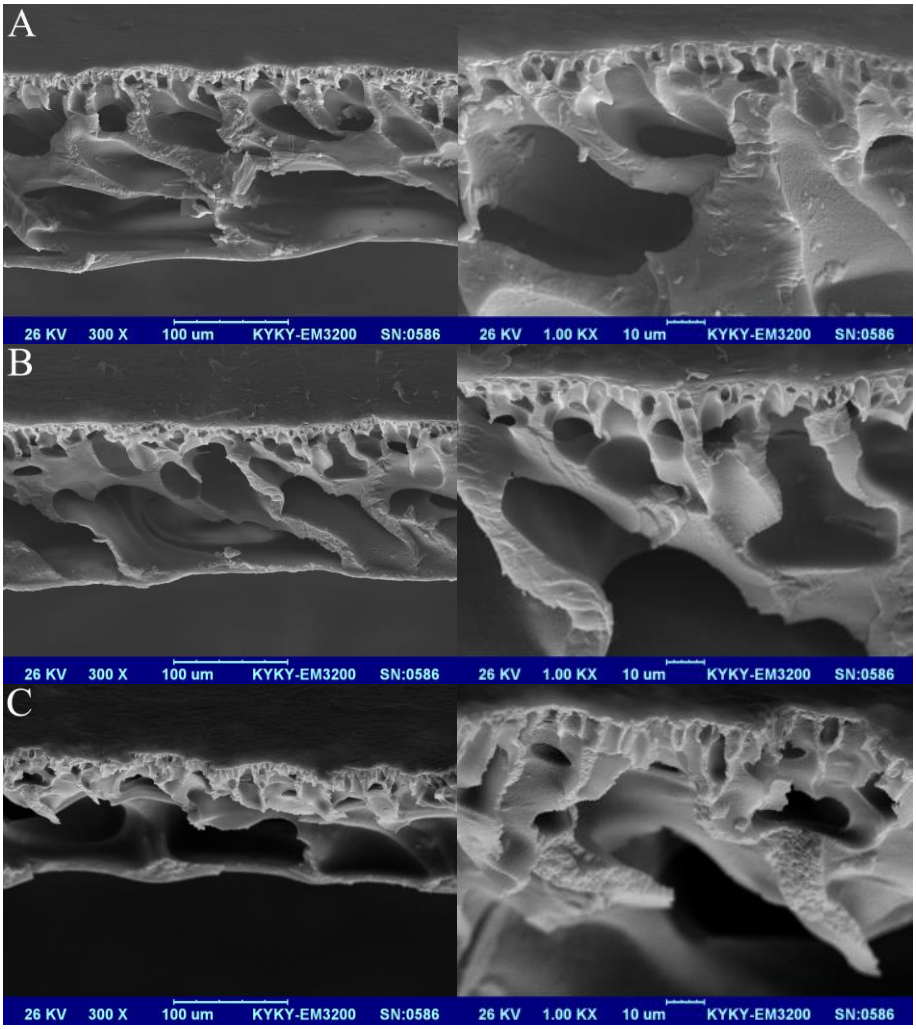

Fig. 1 Cross-section SEM images of waste fiber membranes with different fiber and graphite concentrations (a: 16% wt. waste fibers, b: 16% wt. waste fibers-1% wt. graphite, c: 16% wt. waste fibers-9.4% wt. graphite)

different waste fiber solutions and were cast on glass plate, hydrophobic graphite near the bottom surface of the solutions would shift upwards. This happens to reduce interfacial energy between the hybrid solution and the hydrophilic glass plate. After the hybrid solutions were immersed in water bath, graphite near the top surface of solutions could also shift downwards. Of course, it occurred slowly and was inconsiderable because of the formation of skin layer in the phase separation process. Meanwhile, since the nuclei of polymer poor phase had more water than the surrounding hybrid solutions, graphite powder would recede from the nuclei of polymer poor phase (Zhao, Wang *et al.* 2011). During these movements, a part of layered graphite worked as a grid in front of pores that were being formed. Also, since small graphite powder (1 μm) was ultrasonically dispersed in DMF, an intercalation and exfoliation occurred by the use of solvent and polymer molecules, as might be expected. Amarnath, Hong *et al.* (2011) investigated the effect

of ultrasonic vibrations on the graphite to make graphite nanoplates and Yang, Li *et al.* (2014) exploited ultrasonic cleaner for easily preparing graphene oxide. Ultimately, when the solidification happened, graphite powder was aggregated and stayed in the membranes, thereby causing the formation of membrane structures shown in Fig. 1(b).

These molecular replacements could be verified macroscopically by the color of final hybrid membrane, i.e., the downside of membranes was brighter than the top surface (Fig. SI 3). These photographs illustrated the uniform dispersion of graphite in the horizontal direction of membranes. Also, it shows that these membranes had a multi-layered structure. In SEM images, the graphite powder was not seen. In fact, they cannot be distinguished in the cross-section images, so the final particles should be in the order of nanometers. Based on Amarnath's study, it can be stated that the graphite nanoplates were formed probably in the solvent under ultrasonication. Also, Ballinas *et al*. have described this observation for activated carbon-polysulfone membranes in low loadings (Ballinas, Torras *et al.* 2004, Torras, Ferrando *et al.* 2006). They have claimed that solvating effect occurs between activated carbon and DMF and increases the surface area due to particle channeling (i.e. intercalation and exfoliation). The migration of graphite would leave cavities in the waste fiber membrane matrix, thereby increasing the internal membrane porosity and the interconnection of membrane macrovoids. The formation of nodular structures can happen in the cross-section of these membranes, too. This phenomenon has been observed in many hybrid polymer membranes (Boom, Wienk *et al.* 1992, Smolders, Reuvers *et al.* 1992, Zhu, Xu *et al.* 2007).

When 9.4% wt. graphite powder (>6% wt.) was added to 16% wt. waste fiber solution, the described movements took place during the formation of the hybrid membrane. The structure of this membrane is significantly different (Peng, Lu *et al.* 2005, Lu, Sun *et al.* 2006, Yoshikawa, Shimada *et al.* 2000). This difference was seen for 18% wt. waste fiber solution in the concentration of 5.6% wt. due to the high viscosity of solution. This can provide additional details regarding these hybrid membranes as explained here: Depending on the high weight percent of graphite, they are not really intercalated and exfoliated during the preparation of homogenous waste fiber solutions. They are congregated because of hydrophobicity of them. This was happened during the formation of hybrid ultrafiltration membrane and converting into the coagulation via phase separation. These processes produced some pores that have shown in cross section image (Fig. 1(c)) (Zhao, Wang *et al.* 2011). The surface tension gradient was the main factor in this cross-section structure as developed by Shojaie, Krantz *et al.* (1994a, b). When waste fiber/graphite homogenous solutions with high concentration of graphite were prepared, the interfacial tension gradient was intensely diminished, thereby leading to the formation of many macrovoids. This event was insignificant and unimportant at the low graphite concentration. FT-IR spectra (Fig. SI 3.) were used to confirm the chemical characteristic of industrial graphite powder, waste fiber membrane and waste fiber/graphite hybrid ultrafiltration membrane.

3.2 Performance analysis

In order to select an optimum operating condition and a correct hybrid ultrafiltration membrane for a given hybrid filtration process, the permeate flux, dye rejection and mechanisms of membrane fouling were studied in the cross-flow ultrafiltration setup. The examination of membrane fouling is very important because it provides predictive tools for successful scale up or scale down of ultrafiltration process and minimizes the frequency of backwashing and chemical cleaning (Kim and DiGiano 2009). Therefore, the gradient of flux during a given period (3 hours)

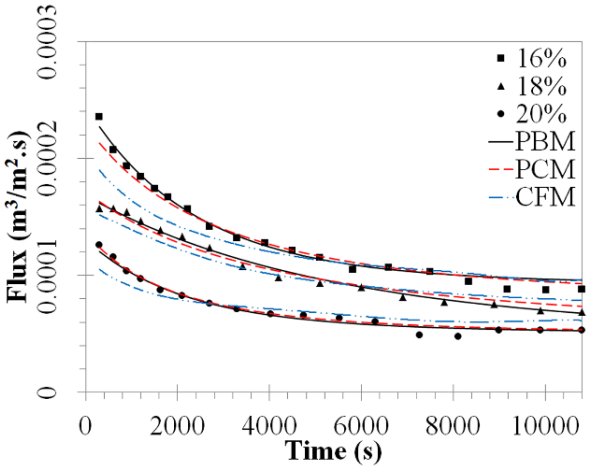

Fig. 2 Time-dependent permeability of waste fiber ultrafiltration membranes prepared from different concentrations with fitted fouling mechanistic models

Table 2 Rejection of Chrysophenine GX of membranes with different waste fiber and graphite powder concentrations

Membranes		Rejection (%)
Waste Fiber	Graphite Powder	
16% wt.	0% wt.	32.2
	1% wt.	56.4
	3% wt.	60.8
	6.3% wt.	59.0
	9.4% wt.	45.0
	12.5 wt.	44.7
	15.6% wt.	32.5
18% wt.	0% wt.	38.4
	1% wt.	60.5
	3% wt.	61.5
	5.6% wt.	50.8
	8.3% wt.	48.5
	11.1 wt.	50.8
20% wt.	0% wt.	43.8
	1% wt.	76.9

was examined for all membranes and the fouling mechanism was achieved via genetic algorithm. As predicted, increasing waste fiber concentration in the dope solution led to a decrease in the permeate flux and an increase in the rejection, as shown in Fig. 2 and Table 2 (Lohokare, Bhole *et al.* 2011, Shinde, Kulkarni *et al.* 1999, Oh, Jegal *et al.* 2001). These variations in the performance could be related to the membrane pore characteristics, i.e., the decrement of pore size and its distribution (Lohokare, Bhole *et al.* 2011, Shinde, Kulkarni *et al.* 1999). Based on Lohokare's

study, it must be also noted that change in the permeate water does not hold a linear relationship with the concentration of the dope solution (Lohokare, Bhole *et al.* 2011).

Kuo and Cheryan (1983) took advantage of power law model to explain the amount of fouling or flux decline; also, this model was introduced as a semi-empirical model by Fane and Fell (1987) (Table 1). If the exponent of this model is small or near zero, the membrane filtration process truly performs the same as the initial flux value and the fouling will be negligible, too. Of course, it must be noted that this model is not a mechanistic model and flux does not approach zero. In real systems, it tends to be a low, but stable, non-zero value (Kuo and Cheryan 1983, Fane and Fell 1987). According to this model, the extent of fouling was high for the membrane with 20% wt. waste fibers and low for 18% wt. membrane (Table SI 1). Fig. 3(a) and (b) obviously illustrate the extent of fouling on the surface of 16 and 18% wt. membranes.

Three flux decline models developed by Field *et al.* were evaluated for all membranes in this study. It is known that these models are only for constant-pressure filtration processes which their streams are cross-flow (Kilduff, Mattaraj *et al.* 2002, Field and Wu 2011). Cross-flow can enhance mass transfer processes that induce back transport from the membrane surface, thereby reducing the net flux of foulant to the membrane surface (Kilduff, Mattaraj *et al.* 2002, Field and Wu 2011). For all membranes, a combination of pore blockage and pore constriction models was dominant and the cake formation model occurred at the last times of ultrafiltration process i.e., > 6000 s (Fig. 2 and Table SI 1). In 18% wt. waste fiber membrane, the blockage of pores took place in the early minutes of filtration process (<3000 s). Furthermore, the large surface pores were constricted at a later time via adhering Chrysophenine GX molecules to their rim and also, through small

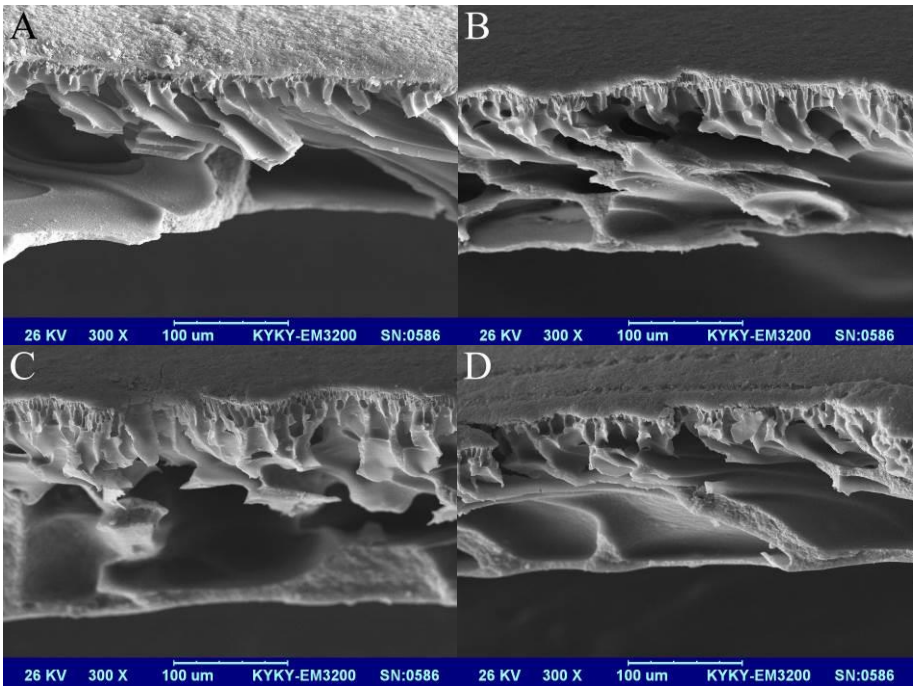

Fig. 3 Cross-section SEM images of fouled waste fiber membranes with different fiber and graphite concentrations (A: 16% wt. waste fibers, B: 18% wt. waste fibers, C: 16% wt. waste fibers-1% wt. graphite powder, D: 18% wt. waste fibers-1% wt. graphite powder)

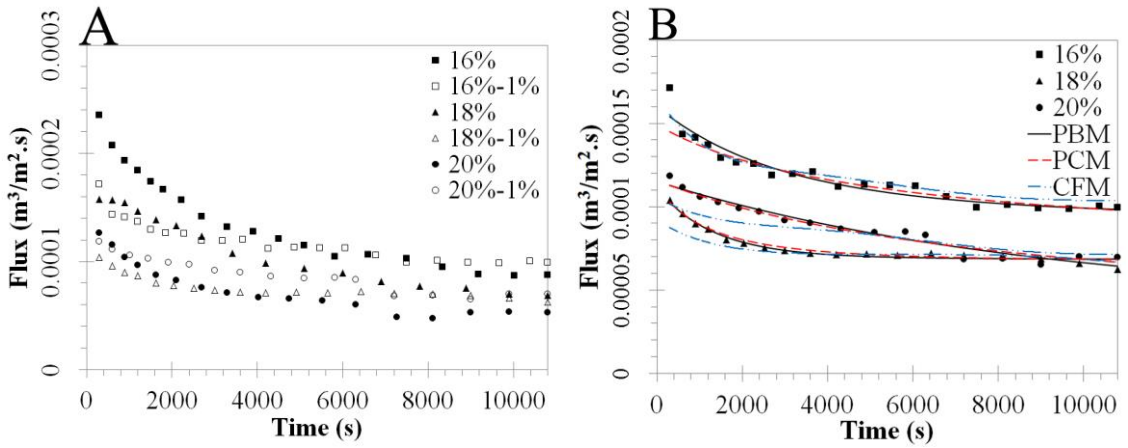

Fig. 4 Time-dependent permeability of membranes prepared from different waste fiber concentrations and 1%wt. graphite powder a: without and b: with fitted fouling mechanistic models

finger-like voids (3000-6000 s). Finally, the cake layer was obtained with smoothing the surface fluctuation irregularly (>6000 s). But, the pore constriction happened first in 16 and 20% wt. membranes (<2000 s) and after that, the pore blockage was done (2000-6000 s). The complete accumulation of dye molecules in small finger-like voids (blue arrow) was significantly observed in 16% wt. waste fiber membrane and the thickness of cake layer (red arrow) was more than 18% wt. waste fiber membrane (Figs. 3(a) and (b)). The 18% wt. waste fiber membrane has the lowest flux decline rate in the early times and the highest decline rate in the late minutes. These properties were in contrast for 16 and 20% wt. waste fiber membranes. It is resulted from the amount of pore blockage parameter and specific cake resistance. With increasing waste fiber concentration, the resistance of membranes is also raised.

By the addition of graphite powder with <6% wt. concentration, the permeate flux is decreased and the rejection of Chrysophenine GX is increased (Fig. 4A, Table 2). These differences are due to the fact that Chrysophenine GX molecules can interact via four ways with these hybrid ultrafiltration membranes to affect their permeate flux and rejection (Peng *et al.* 2005, Yoshikawa *et al.* 2000). 1- Dye molecules with two sulfonate functional groups are adsorbed on the surface of graphite and slightly diffuse in the membrane (the graphite layers are located perpendicular to the membrane surface). 2- Chrysophenine GX is intercalated in the layered graphite that is not free to diffuse and is immobilized. 3- Dye is not intercalated into graphite during the ultrafiltration process. 4- Molecules cannot pass through the parallel graphite layers and subsequently, the membranes.

By the addition of 1% wt. graphite to waste fiber solutions, the membrane fouling was significantly reduced, as shown in Figs. 3(c) and (d) and 4(a). A thin layer of Chrysophenine GX cake was distinguishable on the hybrid ultrafiltration membrane (red arrow). Blending of 1% wt. graphite and 18% wt. waste fiber solution formed a membrane with the lowest fouling among all membranes. This hybrid membrane has the lowest flux decline rate in the early and late times. The overall mechanism of fouling in these membranes was the same as in the membranes without graphite (Fig. 4(b) and Table SI 2). Furthermore, the blockage of pores took place in the early minutes of filtration process (<1800 s for 18% wt.). Afterwards, the pore constriction had the effect at a later time (1800-3400 s for 18% wt.) and the cake layer was finally achieved (>3400 s

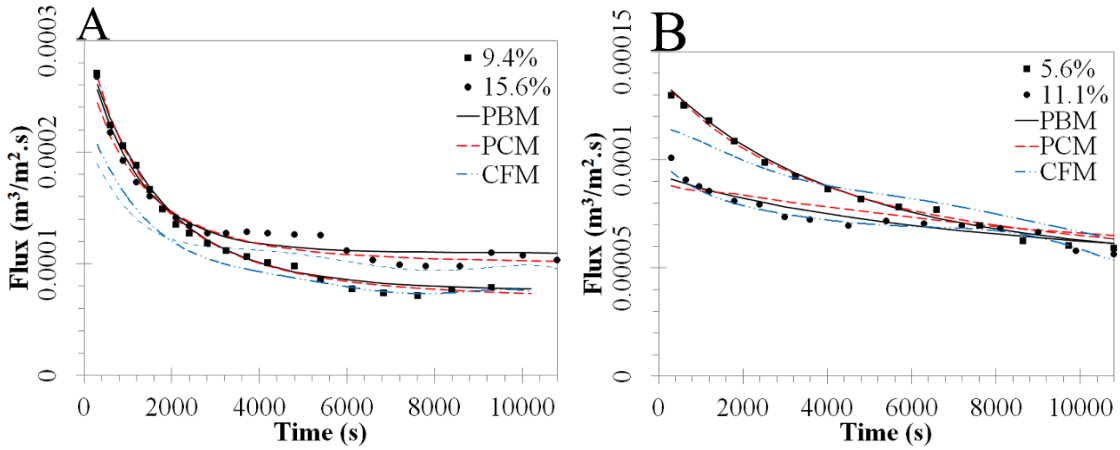

Fig. 5 Time-dependent permeability of membranes prepared from a: 16% wt. and b: 18% wt. waste fiber and different graphite powder concentrations with fitted fouling mechanistic models

for 18% wt.). Moreover, it must be noted that the membrane resistance was improved with the graphite addition in the 18 and 20% wt. waste fiber solutions.

An increment of permeate flux and decrement of Chrysophenine GX rejection is observed when >6% wt. graphite powder was added to waste fibers dope solutions (Fig. 5 and Table 2) (Peng, Lu *et al.* 2005, Lu, Sun *et al.* 2006, Yoshikawa, Shimada *et al.* 2000). These observations are in agreement with the descriptions of SEM images. The fouling of these hybrid membranes was very high and slightly tolerable for 18% wt. waste fiber/5.6% wt. and 11.1% wt. graphite hybrid ultrafiltration membranes (Table SI 3). In all membranes, with the exception of 16% wt. waste fiber/9.4% wt. graphite membrane, the blockage of pores took place in the early minutes of filtration process, the pore constriction had its effect at a later time and finally, the cake layer was achieved (Fig. 5).

Based on Table 2, 16 and 18% wt. waste fiber membranes with 3% wt. graphite powder have higher rejection as compared to 18% wt. waste fiber/1% wt. graphite powder membrane. But, it must be indicated that they have higher membrane fouling dependent upon the exponent of power law model (Table SI 2). Fersi *et al*. utilized the hybrid filtration process included ultrafiltration and nanofiltration for the treatment of dye effluents (Aouni, Fersi *et al.* 2012, Fersi and Dhahbi 2008). In the ultrafiltration process, Everzol Black (MW=991 g/mol) was removed with the rejection of <20% by the use of UF 10 kDa industrial membrane while in this study, Chrysophenine GX (MW=680.66 g/mol) was eliminated with the rejection of 60.5%. Of course, the permeate flux in our cost-efficient membrane was a little low. Also, the performance of optimum hybrid membrane formed in this study for first stage of hybrid membrane filtration process was compared in Table 3 with other methods for Chrysophenine GX removal. The membrane filtration process just had a disadvantage that was the membrane fouling. This disadvantage was significantly reduced in this hybrid membrane. Apparently, 18% wt. waste fiber/1% wt. graphite powder hybrid ultrafiltration membrane has low dye rejection in this comparison, but it was applied in the first stage of treatment process. The pore size distribution of this hybrid membrane is showed in Fig. SI 5. The maximum pore size of this optimum membrane was ranged from 16.10 to 18.72 nm. We are investigating and preparing new nanofiltration membranes for the second stage of Chrysophenine GX elimination process in the laboratory of Dr. Akbari. The hybrid membrane filtration process

Table 3 Comparison of hybrid membrane performance formed in this study with other methods for Chrysophenine GX removal

Methods	Materials	Rejection	Disadvantages	Ref.
Ultrafiltration Process	Waste fibre of mechanized carpet Industrial graphite powder	60.5%	-	this paper
Cloud Point Extraction (CPE)	Triton X-100 as surfactant	96.1% (20 min)	only capable of removing 600 mg/L of dye adding chemical	Abedi and Nekouei (2011)
Photoelectro, Photocatalytic and Chemical Decolourization	CNT as electrode ZnO as nanophotocatalysts Fenton's reagent (H_2O_2 and $FeSO_4$)	92.7% (90 min)	using expensive chemicals high manufacturing and maintenance cost high energy consumption	Khataee and Zarei (2011)
Photo and Chemical Degradation	Fenton's reagent (H_2O_2 and $FeSO_4$)	90% (8 min)	final dangerous volatile products high manufacturing and maintenance cost	Rathi, Rajor *et al*. (2003)
Photocatalytic Degradation	TiO_2 nanoparticles	98.46% (130 min)	high energy consumption long degradation time low pH high energy consumption	Sohrabi and Ghavami (2010)
Biological Treatment	Aerobic granular sludge	86%	long removal time difficult maintenance conditions toxic products	van der Zee, Lettinga *et al*. (2001)
Bioadsorption	Sugarcane bagasse, Propionic acid	55% (25 min)	low pH low efficiency long adsorptive time	Said, Aly *et al*. (2013)
Adsorption	Silver nanoparticles, Activated carbon	~98% (10 min)	using expensive chemicals	Ghaedi, Sadeghian *et al*. (2012)
	Ficus Racemosa L. as activated carbon precursor	91.25% (300 min)	very long adsorptive equilibrium time	Revathi, Ramalingam *et al*. (2011)
	CdO nanowires, Activated carbon	92% (10 min)	using toxic material	Ghaedi, Sadeghian *et al*. (2013)
	Orange peel carbon	96% (120 min)	requiring pre-treatments for long times long removal time very low pH	Khaled, El Nemr *et al*. (2009)

can remove these azo and anionic dye molecules without difficulty and in few minutes. This hybrid membrane was made by the use of inexpensive waste materials and the manufacturing cost is remarkably diminished for this reason. The hybrid membrane filtration processes are more cost-effective and compatible than other methods.

3.3 AFM analysis

To give details of membrane fouling, surface parameters such as average roughness (S_a), root mean square (S_q), peak to peak distance (S_y) and ten point heights (S_z) were measured via atomic

force microscopy. Increasing waste fiber concentration caused a decrease in the average roughness and/or root mean square (Table 4). These results were in agreement with the membrane performance and other researches (Carvalho, Maugeri *et al.* 2011, Stawikowska and Livingston 2013). As mentioned above, 18% wt. waste fiber membrane indicated the least fouling in comparison with others on the own surface. This observation can be described by the height of ten points and the space between the two peaks on the surface. In this membrane, the peak height was small and also, they were located in a short distance from each other, whereas they were dissimilar in 16 and 20% wt. waste fiber membranes (i.e., large peaks and long distances, Fig. 6). As a result, the amounts of accumulated Chrysophenine GX molecules in the valleys were decreased, thereby resulting in valley clogging. Of course, it must be noted that the flow on the surface of this membrane easily created micro or nano-turbulences than other membranes. This causes sweeping of the dye from the surface of membrane and thereby, reducing fouling process (Carvalho, Maugeri *et al.* 2011). Therefore, the coefficient of mass transfer eventually will be increased. In 16% and 20% wt. waste fiber membranes, these turbulence flows could not properly remove the

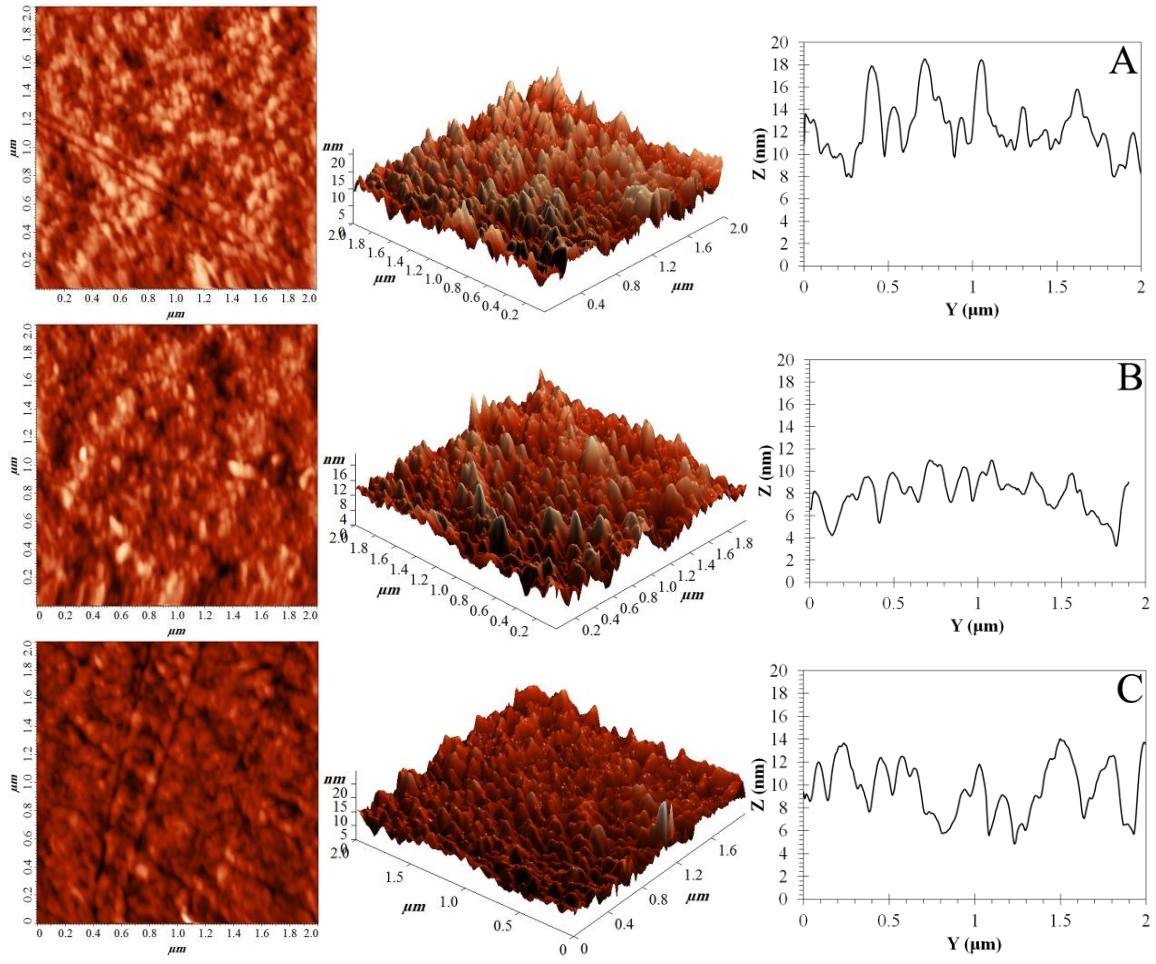

Fig. 6 2D and 3D AFM images and profiles of waste fiber membrane surface with a: 16% wt., b: 18% wt. and c: 20% wt. waste fiber

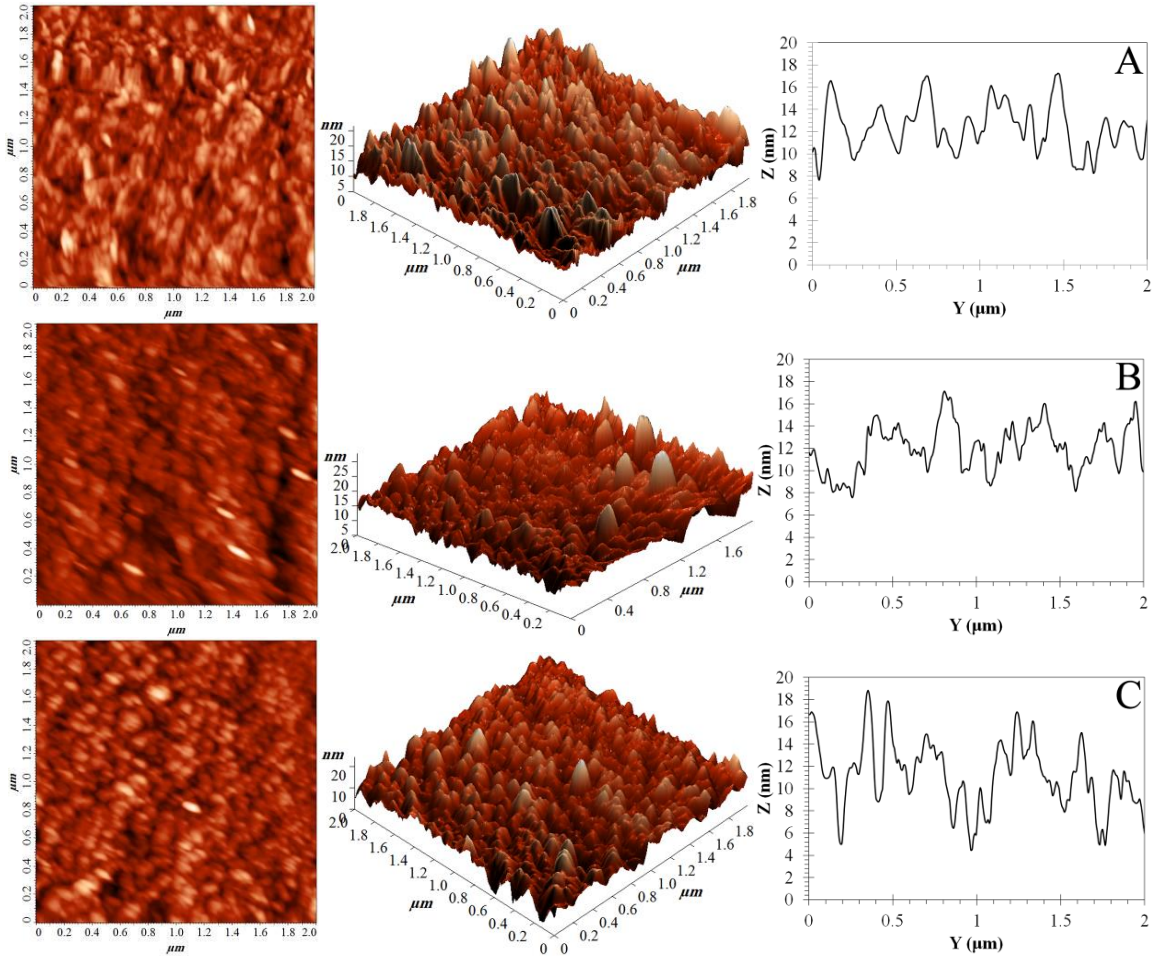

Fig. 7 2D and 3D AFM images and profiles of waste fiber-graphite hybrid membrane surface with a: 16% wt., b: 18% wt. and c: 20% wt. waste fiber and 1% wt. graphite powder

collected dye into the valleys. Hwang and Lin 2002 truly demonstrated the effect of S_z and S_y on the three commercial membranes (MF-Millipore®, Durapore® and Isopore®).

This explanation is clearly compatible with what was mentioned before about fouling mechanism. In 18% wt. waste fiber membrane, the majority of hills and valleys were immediately filled with dye molecules (PBM). Then, the counteraction between the disturbed stream and applied pressure pulled out the more collected molecules from the valleys (not all). Then, the valleys were again filled to a given level (PCM) and after that, the dye elimination was accomplished. Finally, a cake layer was formed on the membrane surface when all of valleys were filled and the turbulent flow could not influence the accumulated molecules (CFM). In other membranes, the valleys were constricted to allowable levels in the early times (PCM). When the valleys were clogged with further dye deposition (PBM), the cross-flow could remove a small part of these amassed. Due to the fact that a lot of Chrysophenine GX molecules were settled into the valleys and turbulent flow could not remove them, the cake layer was easily and quickly formed (CFM).

Table 4 Surface parameters of membranes with different waste fiber and graphite powder concentrations

Membranes	16% wt.				18% wt.				20% wt.	
	0% wt.	1% wt.	9.4% wt.	12.5 wt.	0% wt.	1% wt.	5.6% wt.	11.1 wt.	0% wt.	1% wt.
Peak-to-peak	21.673	21.611	21.735	19.127	19.189	28.007	24.716	55.890	24.902	24.529
Ten point height	11.023	10.818	10.781	9.495	9.588	14.022	12.457	28.082	12.544	12.271
Average roughness	2.033	2.073	2.217	2.144	1.815	2.091	2.223	5.397	1.761	2.079
Root mean square	2.551	2.627	2.765	2.689	2.300	2.716	2.848	6.704	2.248	2.641

The analysis of AFM was accomplished for the hybrid ultrafiltration membranes with 1% wt. graphite powder, i.e., <6% wt. (Table 4 and Fig. 7). It was seen that the average roughness and/or root mean square were unchanged and the properties of membrane fouling could not be considered. Therefore, the height of ten points and the space between two peaks had to be again exploited. As discussed above, the fouling is reduced if S_y and S_z are short and small, respectively. Of course, it must be noted that they have an optimum range (Khulbe, Feng *et al.* 2008). When the peak to peak distance becomes very long, the pore blockage happens fast. In the next minutes, the height of peaks has an effect on constricting the surface pore and the elimination of Chrysophenine GX molecules is facilitated via the cross or turbulent flow. At the end, the cake layer grows and develops on the hybrid ultrafiltration membrane. These two important parameters were almost constant in the 16 and 20% wt. waste fiber/graphite hybrid membranes. The surface parameters of 18% wt. waste fiber membranes without and with 1% wt. graphite powder were located at this optimum range. The results of hybrid ultrafiltration membranes with the concentration of >6% wt. graphite are in accord with the above descriptions and data obtained from AFM as well.

4. Conclusions

The effects of industrial graphite powder on the Chrysophenine GX removal and membrane fouling were investigated and analyzed for Kashan Textile Company. From the present study, the following conclusions can be drawn:

1. With adding graphite powder (<6% wt.), the rejection of hybrid ultrafiltration membranes was improved (32.2 to 56.4% for 16% wt. waste fiber concentration without and with 1% wt. graphite) and the permeate flux was decreased slightly (2.450×10^{-4} to 1.600×10^{-4} $m^3/m^2.s$). The reason for this observation was because of the intercalation and exfoliation of graphite layer which acted as a grid or net in hybrid membranes that were being formed.
2. The fouling mechanism of all membranes resulted from the dominance of pore blockage and constriction at the early time and the cake layer formation at the last times. 18% wt. waste membrane with 1% wt. graphite powder had the minimum fouling.
3. With adding graphite powder (>6% wt.), the performance of these hybrid membranes became worse, i.e., the increment of permeate flux, the decrement of rejection and the deterioration of membrane fouling. This is due to the aggregation of graphite powder in the waste fiber solution and unsuitable intercalation and exfoliation in the ultrasonic bath and agitation of vessel.

4. Among all membranes, the hybrid membrane with the concentration of 18% wt. waste fiber and 1% wt. graphite powder was selected as an optimum hybrid ultrafiltration membrane for removing Chrysophenine GX from dying wastewater. The optimum performance of this membrane was the permeate flux of 1.108×10^{-4} $m^3/m^2.s$, the rejection of 60.5% and low membrane fouling.

References

Abedi, S. and Nekouei, F. (2011), "Removal of direct yellow 12 from water samples by cloud point extraction using triton X-100 as nonionic surfactant", *E-J. Chem.*, **8**(4), 1588-1595.

Adoor, S.G., Sairam, M., Manjeshwar, L.S., Raju, K.V.S.N. and Aminabhavi, T.M. (2006), "Sodium montmorillonite clay loaded novel mixed matrix membranes of poly(vinyl alcohol) for pervaporation dehydration of aqueous mixtures of isopropanol and 1,4-dioxane", *J. Membrane Sci.*, **285**(1-2), 182-195.

Akbari, A., Desclaux, S., Remigy, J.C. and Aptel, P. (2002b), "Treatment of textile dye effluents using a new photografted nanofiltration membrane", *Desalination*, **149**(1-3), 101-107.

Akbari, A., Desclaux, S., Rouch, J.C. and Remigy, J.C. (2007), "Application of nanofiltration hollow fibre membranes, developed by photografting, to treatment of anionic dye solutions", *J. Membrane Sci.*, **297**(1-2), 243-252.

Akbari, A., Desclaux, S., Rouch, J.C., Aptel, P. and Remigy, J.C. (2006), "New UV-photografted nanofiltration membranes for the treatment of colored textile dye effluents", *J. Membrane Sci.*, **286**(1-2), 342-350.

Akbari, A., Remigy, J.C. and Aptel, P. (2002a), "Treatment of textile dye effluent using a polyamide-based nanofiltration membrane", *Chem. Eng. Process.: Process Intensif.*, **41**(7), 601-609.

Allègre, C., Moulin, P., Maisseu, M. and Charbit, F. (2006), "Treatment and reuse of reactive dyeing effluents", *J. Membrane Sci.*, **269**(1-2), 15-34.

Amarnath, C.A., Hong, C.E., Kim, N.H., Ku, B.C. and Lee, J.H. (2011), "Aniline- and N,N-dimethylformamide-assisted processing route for graphite nanoplates: intercalation and exfoliation pathway", *Mater. Lett.*, **65**(9), 1371-1374.

Aouni, A., Fersi, C., Cuartas-Uribe, B., Bes-Pía, A., Alcaina-Miranda, M.I. and Dhahbi, M. (2012), "Reactive dyes rejection and textile effluent treatment study using ultrafiltration and nanofiltration processes", *Desalination*, **297**, 87-96.

Asatekin, A., Olivetti, E.A. and Mayes, A.M. (2009), "Fouling resistant, high flux nanofiltration membranes from polyacrylonitrile-graft-poly(ethylene oxide)", *J. Membrane Sci.*, **332**(1-2), 6-12.

Ballinas, L., Torras, C., Fierro, V. and Garcia-Valls, R. (2004), "Factors influencing activated carbon-polymeric composite membrane structure and performance", *J. Phys. Chem. Solid.*, **65**(2-3), 633-637.

Boom, R.M., Wienk, I.M., van den Boomgaard, T. and Smolders, C.A. (1992), "Microstructures in phase inversion membranes. Part 2. The role of a polymeric additive", *J. Membrane Sci.*, **73**(2-3), 277-292.

Carvalho, A.L., Maugeri, F., Silva, V., Hernández, A., Palacio, L. and Pradanos, P. (2011), "AFM analysis of the surface of nanoporous membranes: application to the nanofiltration of potassium clavulanate", *J. Mater. Sci.*, **46**(10), 3356-3369.

El Nemr, A., Abdelwahab, O., Khaled, A. and El Sikaily, A. (2006), "Biosorption of direct yellow 12 from aqueous solution using green alga Ulva lactuca", *Chem. Ecol.*, **22**(4), 253-266.

Fane, A.G. and Fell, C.J.D. (1987), "A review of fouling and fouling control in ultrafiltration", *Desalination*, **62**, 117-136.

Fathizadeh, M., Aroujalian, A. and Raisi, A. (2011), "Effect of added NaX nano-zeolite into polyamide as a top thin layer of membrane on water flux and salt rejection in a reverse osmosis process", *J. Membrane Sci.*, **375**(1-2), 88-95.

Fersi, C. and Dhahbi, M. (2008), "Treatment of textile plant effluent by ultrafiltration and/or nanofiltration for water reuse", *Desalination*, **222**(1-3), 263-271.

Field, R.W. and Wu, J.J. (2011), "Modelling of permeability loss in membrane filtration: Re-examination of fundamental fouling equations and their link to critical flux", *Desalination*, **283**, 68-74.

Gao, W., Liang, H., Ma, J., Han, M., Chen, Z.L., Han, Z.S. and Li, G.B. (2011), "Membrane fouling control in ultrafiltration technology for drinking water production: A review", *Desalination*, **272**(1-3), 1-8.

Gethard, K., Sae-Khow, O. and Mitra, S. (2010), "Water desalination using carbon-nanotube-enhanced membrane distillation", *ACS Appl. Mater. Interf.*, **3**(2), 110-114.

Ghaedi, M., Sadeghian, B., Kokhdan, S.N., Pebdani, A.A., Sahraei, R., Daneshfar, A. and Mihandoost, A. (2013), "Study of removal of direct yellow 12 by cadmium oxide nanowires loaded on activated carbon", *Mater. Sci. Eng. C*, **33**(4), 2258-2265.

Ghaedi, M., Sadeghian, B., Pebdani, A.A., Sahraei, R., Daneshfar, A. and Duran, C. (2012), "Kinetics, thermodynamics and equilibrium evaluation of direct yellow 12 removal by adsorption onto silver nanoparticles loaded activated carbon", *Chem. Eng. J.*, **187**, 133-141.

Goosen, M.F.A., Sablani, S.S., Al-Hinai, H., Al-Obeidani, S., Al-Belushi, R. and Jackson, D. (2005), "Fouling of Reverse Osmosis and Ultrafiltration Membranes: A Critical Review", *Sep. Sci. Technol.*, **39**(10), 2261-2297.

Huang, H., Qu, X., Dong, H., Zhang, L. and Chen, H. (2013), "Role of NaA zeolites in the interfacial polymerization process towards a polyamide nanocomposite reverse osmosis membrane", *RSC Adv.*, **3**(22), 8203-8207.

Hwang, K.J. and Lin, T.T. (2002), "Effect of morphology of polymeric membrane on the performance of cross-flow microfiltration", *J. Membrane Sci.*, **199**(1-2), 41-52.

Hwang, L.L., Chen, J.C. and Wey, M.Y. (2013), "The properties and filtration efficiency of activated carbon polymer composite membranes for the removal of humic acid", *Desalination*, **313**, 166-175.

Jung, B., Yoon, J.K., Kim, B. and Rhee, H.W. (2004), "Effect of molecular weight of polymeric additives on formation, permeation properties and hypochlorite treatment of asymmetric polyacrylonitrile membranes", *J. Membrane Sci.*, **243**(1-2), 45-57.

Khaled, A., El Nemr, A., El-Sikaily, A. and Abdelwahab, O. (2009), "Treatment of artificial textile dye effluent containing Direct Yellow 12 by orange peel carbon", *Desalination*, **238**(1-3), 210-232.

Khataee, A.R. and Zarei, M. (2011), "Photoelectrocatalytic decolorization of diazo dye by zinc oxide nanophotocatalyst and carbon nanotube based cathode: Determination of the degradation products", *Desalination*, **278**(1-3), 117-125.

Khulbe, K.C., Feng, C.Y. and Matsuura, T. (2008), *Synthetic Polymeric Membranes: Characterization by Atomic Force Microscopy*, Springer-Verlag, Heidelberg.

Kilduff, J.E., Mattaraj, S., Sensibaugh, J., Pieracci, J.P., Yuan, Y. and Belfort, G. (2002), "Modeling flux decline during nanofiltration of NOM with poly(arylsulfone) membranes modified using UV-assisted graft polymerization", *Environ. Eng. Sci.*, **19**(6), 477-495.

Kim, H.J., Choi, K., Baek, Y., Kim, D.-G., Shim, J., Yoon, J. and Lee, J.C. (2014), "High-performance reverse osmosis CNT/Polyamide nanocomposite membrane by controlled interfacial interactions", *ACS Appl. Mater. Interf.*, **6**(4), 2819-2829.

Kim, J. and DiGiano, F.A. (2009), "Fouling models for low-pressure membrane systems", *Sep. Purif. Technol.*, **68**(3), 293-304.

Kim, J. and Van der Bruggen, B. (2010), "The use of nanoparticles in polymeric and ceramic membrane structures: Review of manufacturing procedures and performance improvement for water treatment", *Environ. Pollut.*, **158**(7), 2335-2349.

Koyuncu, I., Topacik, D. and Wiesner, M.R. (2004), "Factors influencing flux decline during nanofiltration of solutions containing dyes and salts", *Water Res.*, **38**(2), 432-440.

Kuo, K.P. and Cheryan, M. (1983), "Ultrafiltration of acid whey in a spiral-wound unit: effect of operating parameters on membrane fouling", *J. Food Sci.*, **48**(4), 1113-1118.

Kurt, E., Koseoglu-Imer, D.Y., Dizge, N., Chellam, S. and Koyuncu, I. (2012), "Pilot-scale evaluation of nanofiltration and reverse osmosis for process reuse of segregated textile dyewash wastewater", *Desalination*, **302**, 24-32.

Lee, J.W., Choi, S.P., Thiruvenkatachari, R., Shim, W.G. and Moon, H. (2006), "Submerged microfiltration

membrane coupled with alum coagulation/powdered activated carbon adsorption for complete decolorization of reactive dyes", *Water Res.*, **40**(3), 435-444.
Li, J.B., Zhu, J.W. and Zheng, M.S. (2007), "Morphologies and properties of poly(phthalazinone ether sulfone ketone) matrix ultrafiltration membranes with entrapped TiO_2 nanoparticles", *J. Appl. Polym. Sci.*, **103**(6), 3623-3629.
Li, J.F., Xu, Z.L., Yang, H., Yu, L.Y. and Liu, M. (2009), "Effect of TiO_2 nanoparticles on the surface morphology and performance of microporous PES membrane", *Appl. Surf. Sci.*, **255**(9), 4725-4732.
Lohokare, H., Bhole, Y., Taralkar, S. and Kharul, U. (2011), "Poly(acrylonitrile) based ultrafiltration membranes: Optimization of preparation parameters", *Desalination*, **282**, 46-53.
Lu, L., Sun, H., Peng, F. and Jiang, Z. (2006), "Novel graphite-filled PVA/CS hybrid membrane for pervaporation of benzene/cyclohexane mixtures", *J. Membrane Sci.*, **281**(1-2), 245-252.
Mirzababaei, M., Miraftab, M., Mohamed, M. and McMahon, P. (2013), "Impact of carpet waste fibre addition on swelling properties of compacted clays", *Geotech. Geol. Eng.*, **31**(1), 173-182.
Nataraj, S.K., Hosamani, K.M. and Aminabhavi, T.M. (2009), "Nanofiltration and reverse osmosis thin film composite membrane module for the removal of dye and salts from the simulated mixtures", *Desalination*, **249**(1), 12-17.
Oh, N.W., Jegal, J. and Lee, K.H. (2001), "Preparation and characterization of nanofiltration composite membranes using polyacrylonitrile (PAN). I. preparation and modification of PAN supports", *J. Appl. Polym. Sci.*, **80**(10), 1854-1862.
Okhovat, A. and Mousavi, S.M. (2012), "Modeling of arsenic, chromium and cadmium removal by nanofiltration process using genetic programming", *Appl. Soft Comput.*, **12**(2), 793-799.
Peng, F., Lu, L., Hu, C., Wu, H. and Jiang, Z. (2005), "Significant increase of permeation flux and selectivity of poly(vinyl alcohol) membranes by incorporation of crystalline flake graphite", *J. Membrane Sci.*, **259**(1-2), 65-73.
Peng, F., Lu, L., Sun, H., Pan, F. and Jiang, Z. (2007), "Organic-Inorganic Hybrid Membranes with Simultaneously Enhanced Flux and Selectivity", *Ind. Eng. Chem. Res.*, **46**(8), 2544-2549.
Prusty, G. and Swain, S.K. (2011), "Synthesis and characterization of conducting gas barrier polyacrylonitrile/graphite nanocomposites", *Polym. Compos.*, **32**(9), 1336-1342.
Purkait, M.K., DasGupta, S. and De, S. (2004), "Removal of dye from wastewater using micellar-enhanced ultrafiltration and recovery of surfactant", *Sep. Purif. Technol.*, **37**(1), 81-92.
Rathi, A., Rajor, H.K. and Sharma, R.K. (2003), "Photodegradation of direct yellow-12 using $UV/H_2O_2/Fe^{2+}$", *J. Hazard. Mater.*, **102**(2-3), 231-241.
Reddy, A.V.R., Trivedi, J.J., Devmurari, C.V., Mohan, D.J., Singh, P., Rao, A.P., Joshi, S.V. and Ghosh, P.K. (2005), "Fouling resistant membranes in desalination and water recovery", *Desalination*, **183**(1-3), 301-306.
Revathi, G., Ramalingam, S., Subramaniam, P. and Ganapathi, A. (2011), "Removal of Direct Yellow-12 Dye from water by adsorption on activated carbon prepared from Ficus Racemosa L.", *E-J. Chem.*, **8**(4), 1536-1545.
Sahoo, G.B. and Ray, C. (2006), "Predicting flux decline in crossflow membranes using artificial neural networks and genetic algorithms", *J. Membrane Sci.*, **283**(1-2), 147-157.
Said, A.A., Aly, A.A., Abd El-Wahab, M.M., Soliman, S.A., Abd El-Hafez, A.A., Helmey, V. and Goda, M.N. (2013), "An efficient biosorption of direct dyes from industrial wastewaters using pretreated sugarcane bagasse", *Energy Environ. Eng.*, **1**(1), 10-16.
Shahnazari, H., Ghiassian, H., Noorzad, A., Shafiee, A., Tabarsa, A.R. and Jamshidi, R. (2009), "Shear Modulus of Silty Sand Reinforced by Carpet Waste Strips", *J. Seismol. Earthq. Eng.*, **11**(3), 133-142.
Shi, Z., Zhang, W., Zhang, F., Liu, X., Wang, D., Jin, J. and Jiang, L. (2013), "Ultrafast separation of emulsified oil/water mixtures by ultrathin free-standing single-walled carbon nanotube network films", *Adv. Mater.*, **25**(17), 2422-2427.
Shinde, M.H., Kulkarni, S.S., Musale, D.A. and Joshi, S.G. (1999), "Improvement of the water purification capability of poly(acrylonitrile) ultrafiltration membranes", *J. Membrane Sci.*, **162**(1-2), 9-22.
Shojaie, S.S., Krantz, W.B. and Greenberg, A.R. (1994a), "Dense polymer film and membrane formation via

the dry-cast process part I. Model development", *J. Membrane Sci.*, **94**(1), 255-280.
Shojaie, S.S., Krantz, W.B. and Greenberg, A.R. (1994b), "Dense polymer film and membrane formation via the dry-cast process part II. Model validation and morphological studies", *J. Membrane Sci.*, **94**(1), 281-298.
Smolders, C.A., Reuvers, A.J., Boom, R.M. and Wienk, I.M. (1992), "Microstructures in phase-inversion membranes. Part 1. Formation of macrovoids", *J. Membrane Sci.*, **73**(2-3), 259-275.
Sohrabi, M.R. and Ghavami, M. (2010), "Comparison of direct yellow 12 dye degradation efficiency using UV/semiconductor and UV/H_2O_2/semiconductor systems", *Desalination*, **252**(1-3), 157-162.
Soleimani, R., Shoushtari, N.A., Mirza, B. and Salahi, A. (2013), "Experimental investigation, modeling and optimization of membrane separation using artificial neural network and multi-objective optimization using genetic algorithm", *Chem. Eng. Res. Des.*, **91**(5), 883-903.
Stawikowska, J. and Livingston, A.G. (2013), "Assessment of atomic force microscopy for characterisation of nanofiltration membranes", *J. Membrane Sci.*, **425-426**, 58-70.
Taşdemır, M., Koçak, D., Usta, İ., Akalin, M. and Merdan, N. (2007), "Properties of Polypropylene Composite Produced with Silk and Cotton Fiber Waste as Reinforcement", *Int. J. Polym. Mater.*, **56**, 1155-1165.
Torras, C., Ferrando, F., Paltakari, J. and Garcia-Valls, R. (2006), "Performance, morphology and tensile characterization of activated carbon composite membranes for the synthesis of enzyme membrane reactors", *J. Membrane Sci.*, **282**(1-2), 149-161.
Van der Bruggen, B., Cornelis, G., Vandecasteele, C. and Devreese, I. (2005), "Fouling of nanofiltration and ultrafiltration membranes applied for wastewater regeneration in the textile industry", *Desalination*, **175**(1), 111-119.
Van der Bruggen, B., Curcio, E. and Drioli, E. (2004), "Process intensification in the textile industry: the role of membrane technology", *J. Environ. Manage.*, **73**(3), 267-274.
Van der Zee, F.P., Lettinga, G. and Field, J.A. (2001), "Azo dye decolourisation by anaerobic granular sludge", *Chemosphere*, **44**(5), 1169-1176.
Yakovlev, A.V., Finaenov, A.I., Yakovleva, E.V. and Finaenova, E.V. (2004), "Use of thermally expanded graphite in water-purification and water-treatment systems", *Russ. J. Appl. Chem.*, **77**(11), 1815-1817.
Yang, H., Li, H., Zhai, J., Sun, L. and Yu, H. (2014), "Simple Synthesis of Graphene Oxide Using Ultrasonic Cleaner from Expanded Graphite", *Ind. Eng. Chem. Res.*, **53**(46), 17878-17883.
Yang, S. and Liu, Z. (2003), "Preparation and characterization of polyacrylonitrile ultrafiltration membranes", *J. Membrane Sci.*, **222**(1-2), 87-98.
Yoshikawa, M., Shimada, H., Tsubouchi, K. and Kondo, Y. (2000), "Specialty polymeric membranes: 12. Pervaporation of benzene-cyclohexane mixtures through carbon graphite-nylon 6 composite membranes", *J. Membrane Sci.*, **177**(1-2), 49-53.
Yunessnia lehi, A., Akbari, A. and Bojaran, M. (2013), "Preparation of nanoporous poly(vinylidene fluoride) membrane and consideration of its performance", *Iran. J. Chem. Chem. Eng.*, **32**(2), 15-29.
Zhao, S., Wang, Z., Wei, X., Tian, X., Wang, J., Yang, S. and Wang, S. (2011), "Comparison study of the effect of PVP and PANI nanofibers additives on membrane formation mechanism, structure and performance", *J. Membrane Sci.*, **385-386**, 110-122.
Zhu, L.P., Xu, L., Zhu, B.K., Feng, Y.X. and Xu, Y.Y. (2007), "Preparation and characterization of improved fouling-resistant PPESK ultrafiltration membranes with amphiphilic PPESK-graft-PEG copolymers as additives", *J. Membrane Sci.*, **294**(1-2), 196-206.

Nomenclatures

A_m Active Permeable Area (m^2)
α Pore Blockage Parameter ($m^2.kg^{-1}$)
α_p Pore Constriction Parameter ($m^3.kg^{-1}$)
α_c Cake Specific Resistance ($m^{-1}.kg^{-1}$)
C_b Bulk Concentration of Solute ($mol.L^{-1}$)
δ_m Membrane Thickness (m)
J Volumetric Flux ($m^3.m^{-2}.s^{-1}$)
J_0 Initial Volumetric Flux ($m^3.m^{-2}.s^{-1}$)
J^* Steady State Volumetric Flux ($m^3.m^{-2}.s^{-1}$)
k Exponent of Power Law Model
N_0 Initial Number of Cylindrical Pores per Unit Membrane Area (pores m^{-2})
r Correlation Coefficient
r_0 Initial Equivalent Radius of Cylindrical Pore (m)
R_m Membrane Resistance (m^{-1})
r_p Equivalent Radius of Cylindrical Pore (m)
t Time (s)

Supporting Information

Fig. SI 1 a: Photographs of initial waste fibers of mechanized carpets before and after washing and drying and b: SEM images of industrial graphite powder

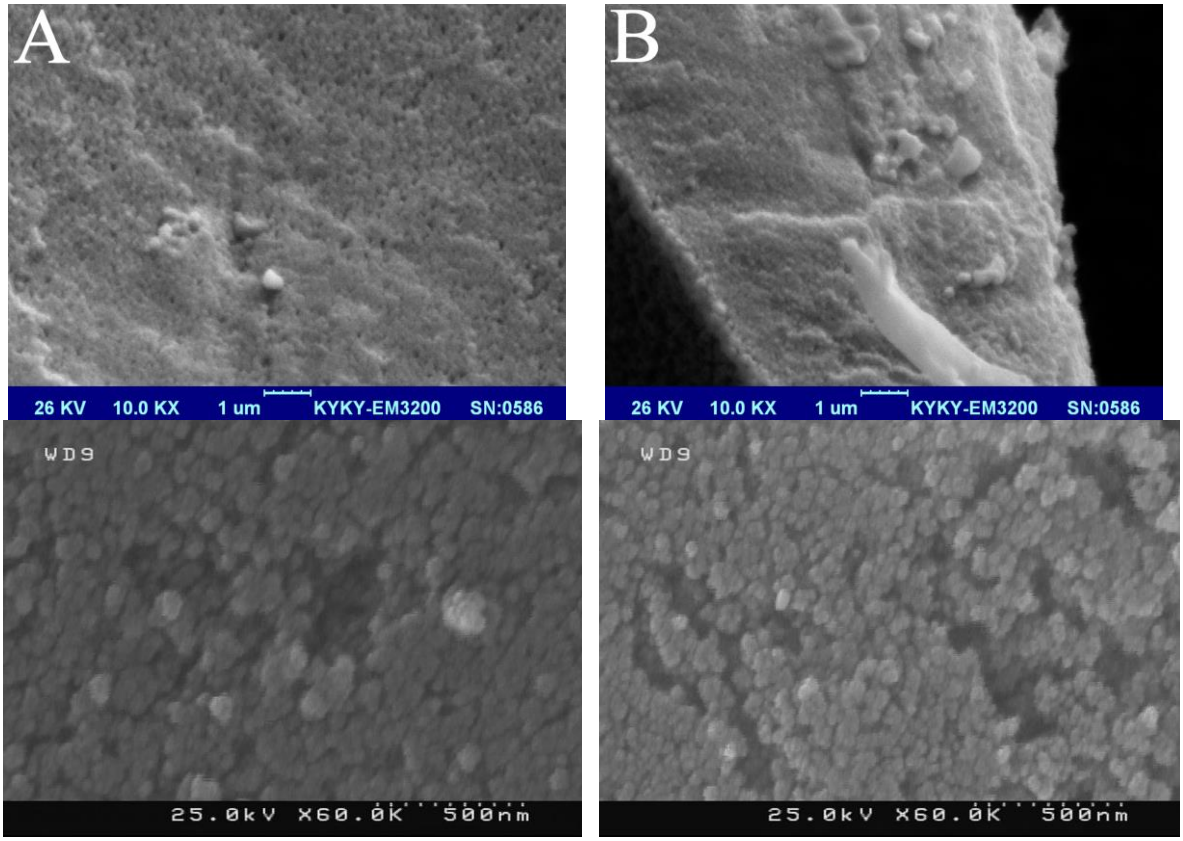

Fig. SI 2 Nodular structures in a: 16% wt. and b: 18% wt. waste fiber membrane

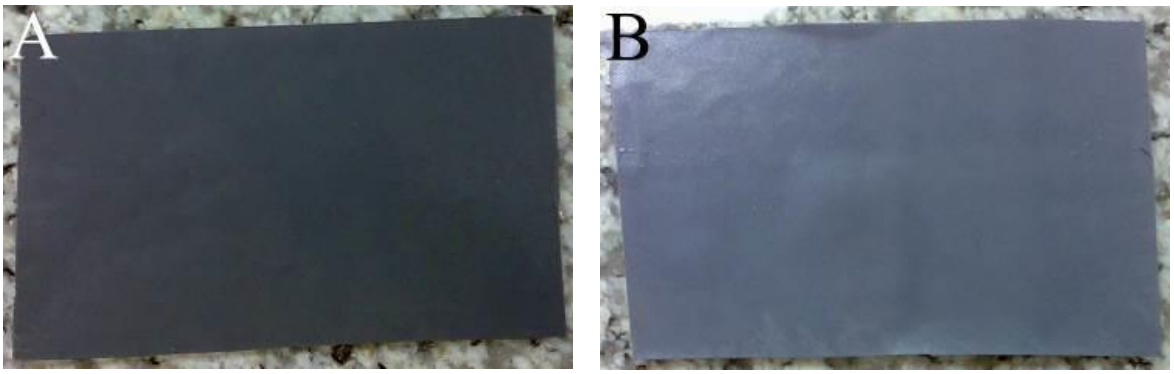

Fig. SI 3 Photograph of a: top layer and b: bottom layer of 16% wt. waste fibers-9.4% wt. graphite hybrid ultrafiltration membrane

The graphite powder showed various major absorption peaks at 3250-3600 cm^{-1} for v_a O-H of alcohol and adsorbed water, 2800-3000 cm^{-1} for v_a C-H of aliphatic carbons, 1633 cm^{-1} for v_a *C=C* of skeletal vibrations from basal graphitic domains, 1400 cm^{-1} for δ C-H of aliphatic carbons, 1123, 1270 cm^{-1} for v_a C-O or C-O-C of alcohol and ether and 557 cm^{-1} for v_a C-C. In this case, several points must be noted: 1- The alcohol and ether functional

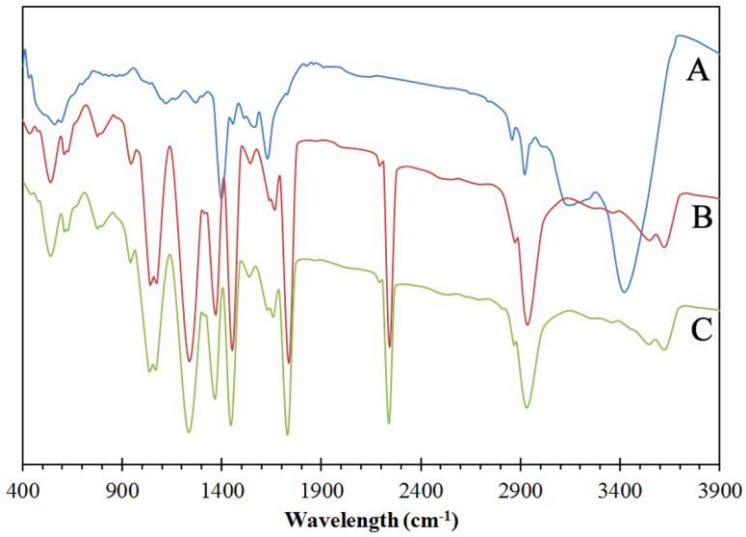

Fig. SI 4 FT-IR spectra of a: industrial graphite powder, b: 16% wt. waste fiber membrane and C: 16% wt. waste fiber-1% wt. graphite hybrid ultrafiltration membrane

Table SI 1 Parameters for cross-flow filtration fouling models with different waste fiber concentrations

Membranes		16% wt.	18% wt.	20% wt.
Power Law Model (PLM)	J_0	3.484×10^{-3}	2.564×10^{-3}	2.584×10^{-3}
	k	0.404	0.392	0.449
	MSE	8.867×10^{-10}	1.122×10^{-9}	3.965×10^{-10}
	r	0.968	0.901	0.970
Pore Blockage Model (PBM)	J_0	2.450×10^{-4}	1.683×10^{-4}	1.304×10^{-4}
	J^*	9.330×10^{-5}	4.816×10^{-5}	4.850×10^{-5}
	α	13.815	7.498	7.649
	MSE	5.681×10^{-11}	1.729×10^{-11}	2.904×10^{-11}
	r	0.990	0.993	0.981
Pore Constriction Model (PCM)	J_0	2.361×10^{-4}	1.720×10^{-4}	1.367×10^{-4}
	J^*	7.364×10^{-5}	4.268×10^{-5}	5.085×10^{-5}
	α_b	5.220	5.605	5.146
	MSE	2.299×10^{-10}	1.289×10^{-10}	2.025×10^{-11}
	r	0.993	0.985	0.986
Cake Formation Model (CFM)	J_0	2.053×10^{-4}	1.567×10^{-4}	1.115×10^{-4}
	J^*	9.173×10^{-7}	1.510×10^{-7}	9.696×10^{-6}
	α_c	1.570	19.144	1.551
	R_m	7.211	13.000	15.952
	MSE	3.174×10^{-10}	6.891×10^{-11}	9.212×10^{-11}
	r	0.879	0.912	0.862

Table SI 2 Parameters for cross-flow filtration fouling models with different waste fiber concentrations and 1% and 3% wt. graphite powder

Membranes		16% wt.		18% wt.		20% wt.
		1% wt.	3% wt.	1% wt.	3% wt.	1% wt.
Power Law Model (PLM)	J_0	1.820×10^{-3}	2.639×10^{-3}	8.046×10^{-4}	0.224	1.457×10^{-3}
	k	0.321	0.381	0.297	0.661	0.345
	MSE	8.083×10^{-10}	5.239×10^{-10}	2.352×10^{-10}	2.721×10^{-9}	6.608×10^{-10}
	r	0.982	0.936	0.985	0.948	0.914
Pore Blockage Model (PBM)	J_0	1.600×10^{-4}	2.099×10^{-4}	1.108×10^{-4}	2.024×10^{-4}	1.151×10^{-4}
	J^*	9.255×10^{-5}	5.558×10^{-5}	6.839×10^{-5}	8.717×10^{-5}	3.811×10^{-5}
	α	8.786	6.305	5.211	8.832	6.144
	MSE	3.008×10^{-11}	2.021×10^{-10}	5.226×10^{-12}	6.823×10^{-11}	1.264×10^{-11}
	r	0.954	0.965	0.977	0.941	0.974
Pore Constriction Model (PCM)	J_0	1.492×10^{-4}	2.083×10^{-4}	1.127×10^{-4}	2.163×10^{-4}	1.158×10^{-4}
	J^*	8.010×10^{-5}	3.338×10^{-5}	6.766×10^{-5}	8.855×10^{-5}	3.678×10^{-5}
	α_b	5.570	5.701	11.170	4.492	5.958
	MSE	4.859×10^{-11}	1.521×10^{-10}	1.148×10^{-11}	7.732×10^{-11}	1.643×10^{-11}
	r	0.939	0.975	0.963	0.940	0.973
Cake Formation Model (CFM)	J_0	1.663×10^{-4}	1.349×10^{-4}	9.212×10^{-5}	1.482×10^{-4}	1.027×10^{-4}
	J^*	2.521×10^{-5}	9.207×10^{-5}	2.220×10^{-16}	2.606×10^{-5}	3.035×10^{-5}
	α_c	8.707	11.358	0.410	15.207	13.245
	R_m	13.551	7.790	11.194	12.020	8.053
	MSE	7.600×10^{-10}	1.629×10^{-9}	7.981×10^{-10}	2.938×10^{-10}	6.816×10^{-10}
	r	0.849	0.884	0.873	0.789	0.903

groups were probably manufactured in the low amount during the production steps. 2- The aliphatic carbons in the graphite may be produced during the degradation of industrial graphite under air (Duquesne, Bras *et al*. 2003). 3- The absorption peak at 1558 cm^{-1} can be related to the vibrations of adsorbed water molecules (Shengtao, Anyan *et al*. 2011). 4- The peak of 3165 cm^{-1} is for KBr powder. Also, the main peaks related to waste fiber membrane (v_a (O-H, confined water in the small pores or adsorbed water on the membrane surface): 3630 cm^{-1}, v_a (C-H, aliphatic chain): 2934 cm^{-1}, v_a (C≡N, acrylonitrile monomer): 2243 cm^{-1}, v_a (C=O, esteric carbonyl of methyl acrylate monomer): 1737 cm^{-1}, v_a (C=C, unreacted acrylic monomers): 1666 cm^{-1}, δ (C-H, sp^3 aliphatic chain): 1450, 1370, 770 cm^{-1}, v_a (C-O-C, methyl acrylate monomer): 1234, 1035 cm^{-1}, δ (C-H, sp^2 aliphatic chain): 940 cm^{-1} and v_a (C-C, aliphatic chain): 607, 538 cm^{-1}) were truly indicated. The IR spectrum of waste fiber-graphite hybrid membrane was so familiar with waste fiber membrane. The graphite has no chemical effects on the waste fiber membrane.

Duquesne, S., Bras, M.L., Bourbigot, S., Delobel, R., Vezin, H., Camino, G., Eling, B., Lindsay, C. and Roels, T. (2003), "Expandable graphite: a fire retardant additive for polyurethane coatings", *Fire Mater*., **27**(3), 103-117.

Shengtao, Z., Anyan, G., Huanfang, G. and Xiangqian, C. (2011), "Characterization of exfoliated graphite prepared with the method of secondary intervening", *Int. J. Ind. Chem.*, **2**(2), 123-130.

Table SI 3 Parameters for cross-flow filtration fouling models with 16 and 18% wt. waste fiber and different graphite concentrations

Membranes		16% wt.				18% wt.		
		6.3% wt.	9.4% wt.	12.5% wt.	15.6% wt.	5.6% wt.	8.3% wt.	11.1% wt.
Power Law Model (PLM)	J_0	3.670×10^{-3}	1.624×10^{-2}	1.828×10^{-2}	2.940×10^{-3}	1.914×10^{-3}	0.222	1.526×10^{-3}
	k	0.458	0.626	0.604	0.395	0.377	0.969	0.379
	MSE	1.162×10^{-9}	2.178×10^{-9}	4.027×10^{-9}	3.432×10^{-10}	7.924×10^{-10}	3.192×10^{-9}	6.151×10^{-10}
	r	0.926	0.964	0.917	0.989	0.920	0.968	0.951
Pore Blockage Model (PBM)	J_0	1.334×10^{-4}	2.971×10^{-4}	3.220×10^{-4}	2.982×10^{-4}	1.381×10^{-4}	1.829×10^{-4}	9.294×10^{-5}
	J^*	3.958×10^{-5}	7.462×10^{-5}	5.885×10^{-5}	1.093×10^{-4}	5.210×10^{-5}	6.858×10^{-5}	3.817×10^{-5}
	α	27.005	6.957	7.973	9.333	8.522	7.089	23.247
	MSE	2.708×10^{-10}	8.834×10^{-11}	4.830×10^{-11}	9.182×10^{-11}	1.737×10^{-11}	2.171×10^{-11}	2.705×10^{-11}
	r	0.983	0.988	0.995	0.976	0.993	0.985	0.938
Pore Constriction Model (PCM)	J_0	1.458×10^{-4}	3.152×10^{-4}	3.156×10^{-4}	2.866×10^{-4}	1.383×10^{-4}	1.813×10^{-4}	8.939×10^{-5}
	J^*	3.402×10^{-5}	6.948×10^{-5}	4.303×10^{-5}	1.009×10^{-4}	4.947×10^{-5}	6.794×10^{-5}	3.009×10^{-5}
	α_b	6.130	3.110	4.570	4.762	3.749	5.979	11.881
	MSE	1.574×10^{-10}	3.754×10^{-11}	6.315×10^{-10}	9.667×10^{-11}	1.597×10^{-11}	4.480×10^{-11}	4.713×10^{-11}
	r	0.981	0.995	0.986	0.974	0.992	0.977	0.934
Cake Formation Model (CFM)	J_0	1.319×10^{-4}	2.332×10^{-4}	2.241×10^{-4}	2.154×10^{-4}	1.153×10^{-4}	1.172×10^{-4}	1.003×10^{-4}
	J^*	3.151×10^{-5}	5.544×10^{-6}	2.564×10^{-5}	3.703×10^{-5}	6.605×10^{-5}	1.003×10^{-5}	6.250×10^{-5}
	α_c	12.045	3.226	0.508	0.973	16.642	13.628	8.657
	R_m	15.954	19.862	19.004	16.871	2.503	13.530	9.866
	MSE	8.595×10^{-10}	5.683×10^{-10}	2.372×10^{-9}	6.761×10^{-10}	2.002×10^{-9}	1.959×10^{-10}	1.381×10^{-9}
	r	0.896	0.729	0.905	0.739	0.893	0.898	0.876

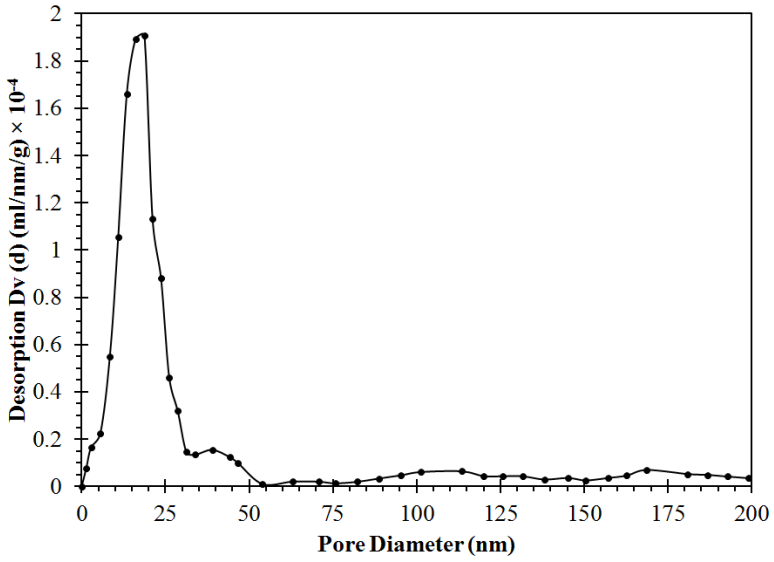

Fig. SI 5 Pore size distribution of optimum hybrid ultrafiltration membrane (18% wt. waste fiber-1% wt. industrial graphite powder)